ELSEVIER

Journal of Alloys and Compounds 281 (1998) 280–289

Journal of ALLOYS AND COMPOUNDS

Phase development and kinetics of high temperature Bi-2223 phase

Mustafa Yavuz[a,*], Hiroshi Maeda[a], Lou Vance[b], Hua Kun Liu[c], Shi Xue Dou[c]

[a]*Tohoku University, Institute for Materials Research (IMR), Katahira 2-1-1, Sendai 980-77, Japan*
[b]*Advance Materials, Australian Nuclear and Technology Organisation (ANSTO) Lucas Heights, Private Mail Bag 1, Menai, NSW 2234, Australia*
[c]*Centre for Superconducting and Electronic Materials University of Wollongong, Northfields Avenue, Wollongong, NSW 2500, Australia*

Received 12 June 1998; received in revised form 6 July 1998

Abstract

The two-dimensional nucleation (random)-growth mechanism were observed as a support for the related previous works, which is attributable to the growth of the Bi-2223 grain in the *a–b* plane direction of the Bi-2212 matrix is being much faster than in the c-direction, or that the early-formed plate-like 2212 phase confines the 2223 product. At the beginning of the reaction, the additional phases are partially melted. Because of the structure, composition and thermal fluctuation, the 2223 nucleates and grows in the phase boundary between the liquid phase and Bi-2212. It was shown here that the nucleation and the growth rate were relatively fast between 0 and 36 h. At the final stage, between 36 and 60 h, because of the impingement of the growth fronts of different nuclei, the high formation rate of 2223 is suppressed. The major reactant 2212 remains as a solid and its plate-like configuration determines the two dimensional nature of the reaction. The amount of liquid forms during reaction is small.

Keywords: High-T_c superconductivity; Phase formation and kinetics

1. Introduction

There have been several proposals regarding the formation mechanisms of the (Bi,Pb)-2223 phase, but the exact mechanism is not yet known. In general, the different mechanisms proposed can be categorised as: A liquid phase related to Ca_2PbO_4 is proposed to be present; (Bi,Pb)-2223 then forms by a disproportionation reaction [1] involving PbO flux [2] or a reaction between 2212 and the liquid phase [3–8]; Ca_2PbO_4-related liquid phase is again proposed to be present; the liquid phase is related to the melting of 2212; (Bi,Pb)-2223 forms by a precipitation process [9,10]; No liquid is required to form (Bi,Pb)-2223; (Bi,Pb)-2223 forms by an insertion process where the Ca, Cu and O diffuse into the Bi-2212 phase and it converts to Bi-2223 phase [11–25]. Komatsu et al. [19] and Mizuno et al. [11] found that Pb acts as flux for the formation of high T_c-phases; The addition of Pb, combined with excess Ca, leads to the formation of Ca_2PbO_4, which acts as a reservoir for Ca and prevents PbO from acting as a flux [17]. The formation of the Ca_2PbO_4 phase produces partially melted materials (non-superconducting phases such as Ca_2CuO_3 and $Sr_{14}Cu_{24}0_{41}$), offers a fast reaction path to form 2223 [10], and accelerates the formation of 2212 phase [26–30]. Ca_2PbO_4 decomposes or melts around at 825°C in the presence of 2212 phase [31] (note that Kitaguchi et al. [32] reported that Ca_2PbO_4 by itself is stable (up to 980°C in air), and widens and lowers the temperature range of partial melting. The liquid enhances dissolution of the 2212 phase as well as other unwanted phases [10]; Pb can substitute for Bi in the crystal structure of the 2223 phase [28]. The volume fraction of the 2223 phase increases with increasing Pb, but excess Pb lowers the formation temperature of intermediate species and forms strontium-lead oxide as a new intermediate phase [16]; According to Wong–Ng et al. [26], relative to the exact 2223 stoichiometry, excess amounts of Ca and Cu are needed for the formation of significant quantities of 2223. However, Chen et al. [4,6] found that the optimum composition which maximises the 2223 formation should be stoichiometric in Ca and Cu, but contain a slight excess of Pb.

All the proposed (Bi,Pb)-2223 formation mechanisms, except for the insertion mechanism, appear to depend on the presence of a liquid phase, but even the insertion process could be facilitated by faster cation diffusion in a liquid. Therefore, it appears that understanding the (Bi,Pb)-2223 formation mechanism can be furthered by elucidating the role Ca_2PbO_4 plays in forming (Bi,Pb)-2223 and the source of liquid phase.

*Corresponding author.

0925-8388/98/$ – see front matter
PII: S0925-8388(98)00795-6

This work concentrates on high-T_c (2223) phase formation and its formation mechanisms during heat treatment of freeze-dried nitrate-route material. The high-T_c phase formation kinetics were analysed using the Avrami relation for the isothermal phase transformations [33,34].

The Avrami equation, which has been found to be well suited to describe the (Bi,Pb)-2223 phase formation [34], is expressed as follows:

$$C = 1 - \exp(-kt^n) \quad (1)$$

where C is the volume fraction of the sample transformed into (Bi,Pb)-2223, k is the rate constant, t is the time at the reaction temperature and n is an exponent (the Avrami exponent), dependent on the nature and the characteristics of the transformation. According to Rao and Rao [35], in the case of diffusion-controlled transformations, the exponent n can take values as: (a) $n=2.5$: initial growth of particles nucleated at constant rate, (b) $n=1.5$: initial growth of particles nucleated only at the start of the transformation, (c) $n=1$: growth of isolated plates or needles of finite size, (d) $n=0.5$: thickening of plates after their edges have impinged.

It is important to note that the value of n is subject to variations in the transformation conditions, making it difficult to directly compare the n values determined by different authors under various experimental conditions.

In Eq. (1), the reaction rate obeys an Arrhenius type of relation [36]:

$$k = k_0 \exp(E_{act}/RT) \quad (2)$$

where k_0 is a constant, E_{act} is the activation energy for the 2223 phase formation, R is the gas constant and T is the absolute temperature.

Substituting Eq. (2) into Eq. (1) and rearranging the terms gives,

$$\ln[-\ln(1-C)] = (\ln k_0 - Q/RT) + n \ln t \quad (3)$$

At a given temperature, the first term of the right side of equation is a constant. The theoretical analysis of Avrami is based on the assumption that germ nuclei from which the new phase is nucleated are already present and randomly distributed in the sample at the time taken as $t=0$.

Sung and Hellstrom [31] analysed the kinetics of forming (Bi,Pb)-2223 from a mixture of 2212 and non-superconducting phases, mainly Ca_2PbO_4 and CuO, using Avrami analysis [33,37,38]. They concluded that the kinetics were described by a diffusion-controlled two dimensional nucleation and growth process. They found a large apparent activation energy for forming (Bi,Pb)-2223, 890 kJ mol^{-1} above 825°C and 2500 kJ mol^{-1} below 825°C in 7.5% O_2/Ar. Liquid formation above 825°C appeared to be vital for speeding up the formation kinetics. These results also are in good agreement with those obtained by Grivel and Flukiger [36]. They have found that increasing the temperature at which the precursor powders are calcined results in a lowering of the apparent Eact, and a longer holding time at the chosen sintering temperature results in a lowering of the apparent E_{act}, due to the smaller contribution of the partial melting reaction to the overall process.

2. Experimental

$Bi_{1.84}Pb_{0.35}Sr_{1.95}Ca_{2.05}Cu_{3.05}O_y$ ceramics were prepared using the freeze-dry method. Metal nitrate solutions were made by weighing and dissolving $Bi(NO_3)_{3.5}H_2O$ in ~3 mol l^{-1} nitric acid; $Pb(NO_3)_2$, $Sr(NO_3)_2$, $Ca(NO_3)_{2.4}H_2O$, $Cu(NO_3)_2.2.5H_2O$ in distilled water; and mixing the five solutions in the cation ratio Bi/Pb/Sr/Ca/Cu=1.84/0.35/1.91/2.05/3.05 [39–41]. The resultant nitrate-solution was fed into the spray-dry machine (Yamato, Model GA-32), which was used as an atomiser for the solution before being fed in to the freeze-dry machine (Labconco Freeze-dry system, Freeze Zone 4.5). The nitrate solution was atomised into a stainless-steel thermos containing liquid nitrogen. The frozen powder was then transferred to the freeze-dry machine pre-set to a temperature of −45°C and operated at a pressure of 0.1 Pa. The sample temperature and chamber pressure were continuously monitored and the temperature was raised to 20°C over a period of one day. The dried powders were transferred into an alumina crucible, placed in a muffle furnace preheated to 250°C for an hour, and calcined at 770°C in the muffle furnace for nearly 15 h in air, hand ground by alumina mortar and pestle for 5 min, pressed into pellets using 3 tons pressure, and sintered in air at 850°C for various times. The heat-treated samples were characterised by SEM, XRD and ICP chemical analysis. The bulk Bi–Pb–Sr–Ca–Cu–O samples were polished but not etched and mounted in a polymeric container and C-coated for the back and secondary scattering SEM.

The XRD technique has been used to estimate the phase composition of the superconducting system [15,34,42–45]. For the Bi-2223 system, the ratio I_{2223} (00$\underline{10}$)/[I_{2212} (008)+I_{2223} (00$\underline{10}$)], where I is the intensity of the XRD peaks, was used for this purpose. It was also employed here to detect the volume fraction of the 2223 phase for different sintering times.

3. Results and discussion

The high reactivity of freeze-dried precursors is seen from the formation of a large fraction of 2223 (91%) after holding for 60 h at 850°C (solubility of Pb in the 2223 phase is a maximum at 850°C [46]) (see Fig. 1). The advantages of this process over conventional oxide routes and some other chemical routes have been described in previous works of the authors [39–41].

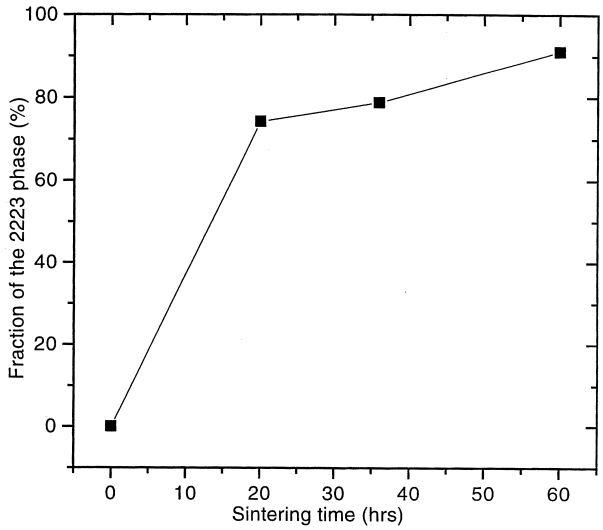

Fig. 1. High-T_c phase volume fraction as a function of sintering time at 850°C in air for the pelletised bulk Bi–Pb–Sr–Ca–Cu–O superconductors prepared from freeze-dried precursor powders.

According to K. Schultze at al. [47], the equilibrium phase reaction of the unleaded Bi_2O_3–SrO–CaO–CuO system with a chemical composition of the Bi-2223 phase at 850°C is

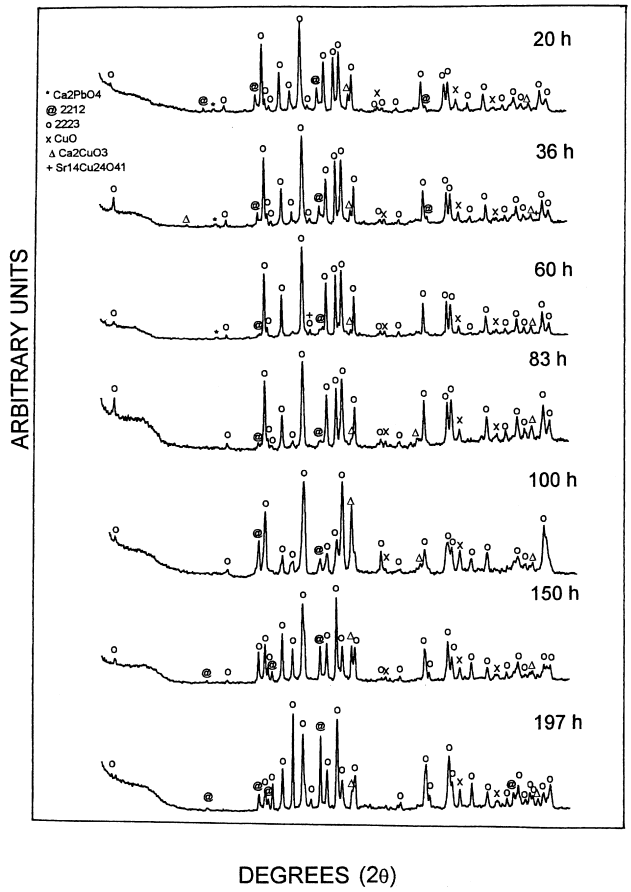

Fig. 2. XRD patterns of freeze-dried bulk Bi–Pb–Sr–Ca–Cu–O samples sintered at 850°C for various times.

Table 1
High-T_c phase volume % and cation ratios as function of sintering time obtained using chemical analysis through icp-aes

Sintering time (h)	Sr/Ca	Cu/Sr	Bi/Pb	2223%
0	0.96	1.51	4.72	0
20	0.96	1.49	4.84	74.28
36	0.92	1.46	4.84	78.8
60	1.00	1.53	5.11	91
83	0.95	1.47	5.26	83.8
100	1.00	1.47	5.11	58.7
150	0.91	1.46	5.41	54.4
197	0.87	1.67	5.46	53.7
theoretical	0.93	1.60	5.26	–

$$Bi-2212 + 1/2Ca_2CuO_3 + 1/2CuO = Bi-2223 \quad (4)$$

If the chemical composition of the superconducting precursor is close to stoichiometric Bi-2223 and the starting phases of the calcined and/or sintered samples are mainly Bi-2212 [39,41] and the other non-superconducting phases [10,48–51]:

$$Bi-2212 + SP = Bi-2223 \quad (5)$$

where SP denotes the non-superconducting phases, in addition to Bi-22 12. When PbO is added, the cations, Ca^{2+} and Cu^{2+}, in the melt can be quickly transported to the surface of Bi-2212, where the Bi-2223 phase nucleates and grows. In other words, the Ca_2CuO_3 improves the cation diffusion and accelerates the chemical reaction. It is suggested here that, during formation of the 2223 phase, Ca_2PbO_4 acts like a catalyst, assisting the melting process and speeding up the growth of the 2223 phase in such a way that Ca_2PbO_4 produces a lead-rich liquid phase and CaO at a temperature above its melting point (Eq. (6)).

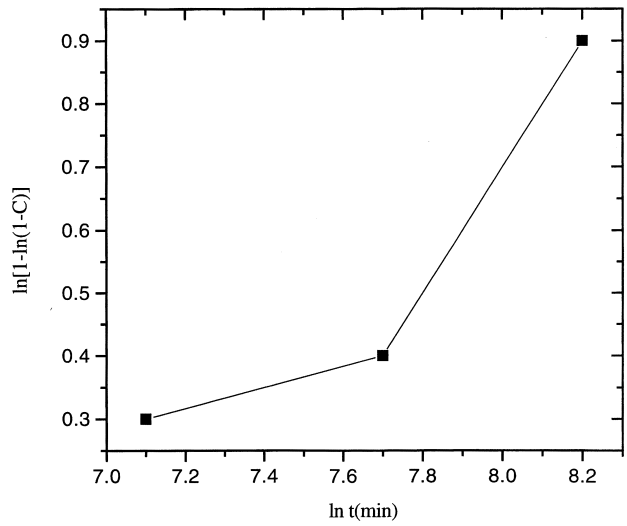

Fig. 3. Plot of ln(−ln(1−C)] versus ln t for the high-T_c phase formation for the bulk Bi–Pb–Sr–CaCu–O superconductors prepared from the freeze-dried precursor powders.

Table 1 shows that the Bi/Pb ratio increased to 4.84 from its starting value of 4.72 after 20 h sintering, remained constant at 36 h, and increased to 5.11 after 60 h. Thus there was no significant change occurred during prolonged sintering, but only a small amount of evaporation (~8%), suggesting that Pb in the form of Ca_2PbO_4 is participating in the nucleation process for 2223 phase and its influence on the growth of 2223 phase is not substantial as Ca^{2+} and Cu^{2+}. Within the lead-rich phase, the rate of interdiffusion among the 2212 phase, Ca_2CuO_3 and CuO, can be increased beyond that of solid-state diffusion if a liquid phase is present. Therefore, the Eq. (4) becomes

$$\begin{aligned} &Bi_2Sr_2CaCu_2O_8\ (\text{reacted}) + Ca_2CuO_3\ (\text{reacted}) \\ &\quad + CuO\ (\text{reacted}) + Ca_2PbO_4\ (\text{reacted}) \\ &= (Bi,Pb)_2Sr_2Ca_2Cu_3O_{10} + Sr_{14}Cu_{24}O_{41} \\ &\quad + Ca_2PbO_4\ (\text{unreacted}) + CuO\ (\text{unreacted}) \\ &\quad + Ca_2CuO_3\ (\text{unreacted}) + Bi_2Sr_2CaCu_2O_8\ (\text{unreacted}) \end{aligned} \quad (6)$$

where Ca_2PbO_4 (reacted)–Ca_2PbO_4 (unreacted) [41]. XRD patterns in Fig. 2 clearly show that non-superconducting phases such as CuO, Ca_2CuO_3, Ca_2PbO_4 and $Sr_{14}Cu_{24}O_{41}$ are present during and after the formation of the 2223 phase (20, 36, and 60 h sintering). This result also confirms work done by Majewski [52] who has determined four- and five-phase regions of phases present such as 2223, Ca_2CuO_3, CuO, Ca_2PbO_4, and $5r_{14}Cu_{24}O_{41}$. Table 1 shows the variation of the Sr/Ca, Cu/Sr and Bi:Pb ratios as a function of sintering time at 850°C. The Sr/Ca and Cu/Sr ratios decreased during 20 and 36 h sintering. It is emphasised that the 2223 phase is in equilibrium with Ca_2CuO_3 and Ca_2PbO_4 (Fig. 2). After 60 h of sintering, the Sr/Ca ratio increased rapidly and reached a maximum value of 1.00, and the Cu/Sr ratio increased from 1.46 to 1.53, indicating the 2223 phase is in equilibrium mainly with $Sr_{14}Cu_{24}O_{41}$ and CuO (Fig. 2), where the lattice parameters were obtained as $a=3.779$, $b=3.834$, and $c=37.154$ Å s with wavelength Cu K$\alpha=1.542$ Å (Table 2).

During the decomposition of the 2223 phase, the Sr/Ca

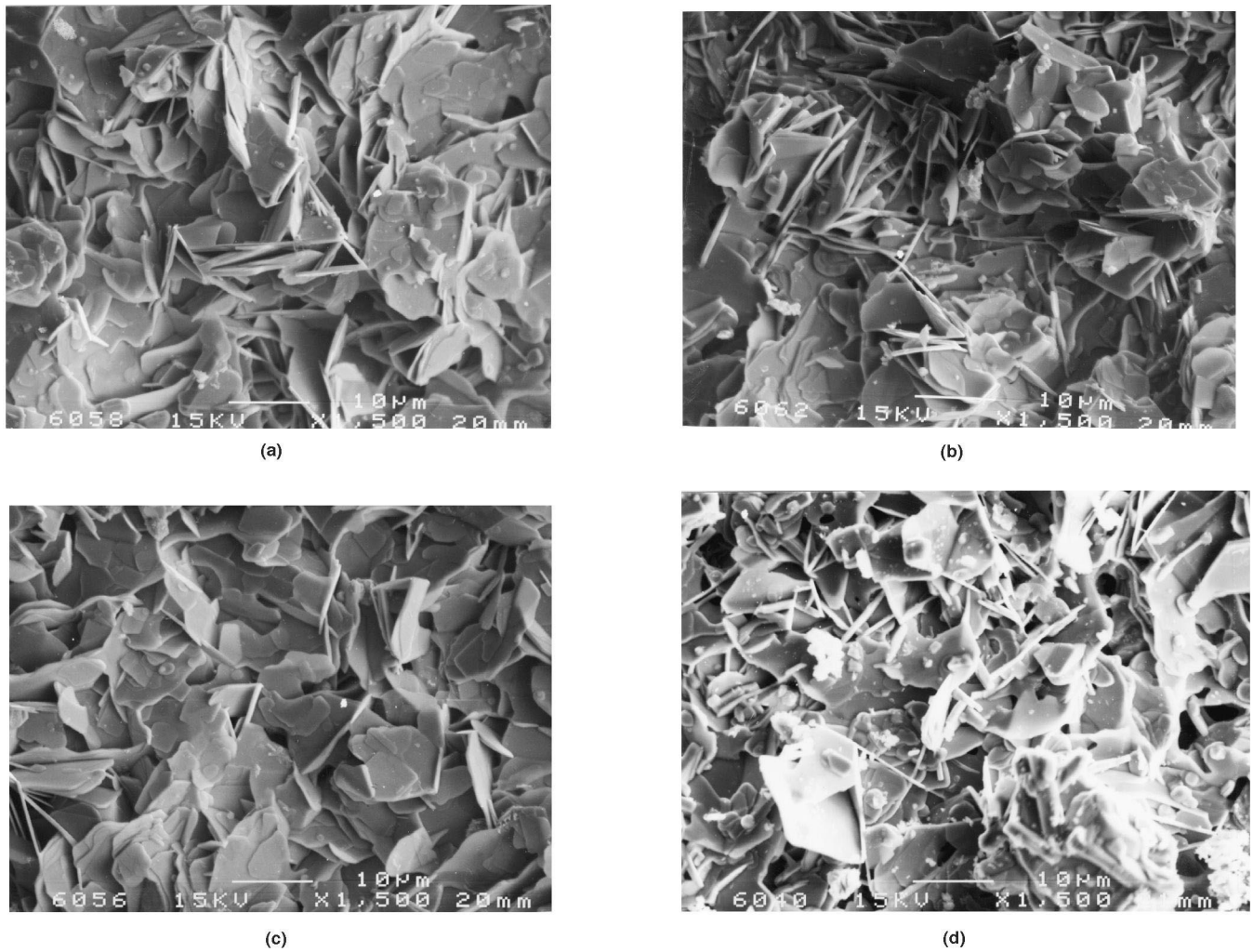

Fig. 4. SEM micrographs of the bulk Bi–Pb–Sr–Ca–Cu-superconductors prepared from the freeze-dried precursor powders sintered at 850°C in air for (a) 20 h, (b) 36 h, (c) 60 h, (d) 83 h, (e) 100 h, 150 h, (g) 197 h.

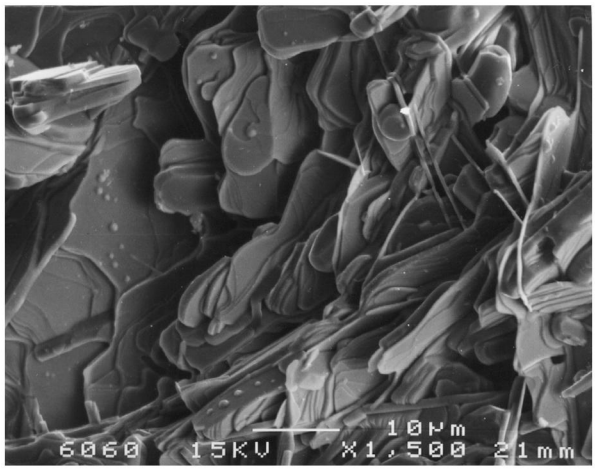

(e)

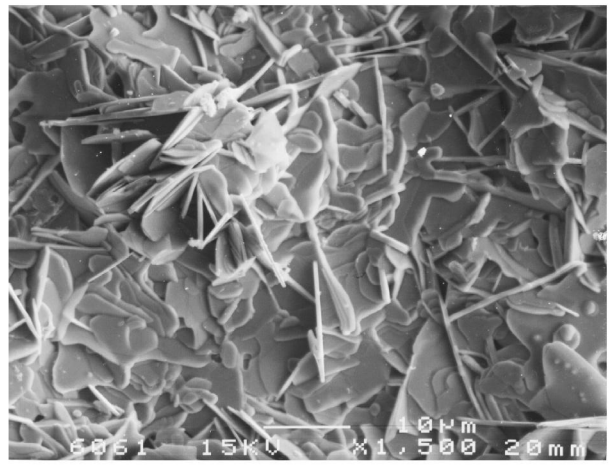

(f)

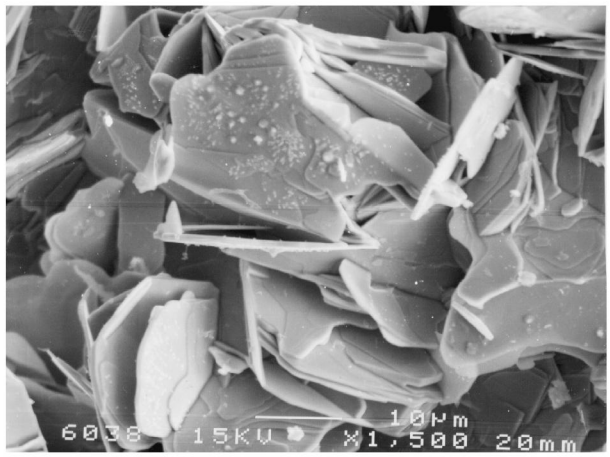

(g)

Fig. 4. (*continued*)

and the Cu/Sr ratios decreased from 1.00 to 0.95 and from 1.53 to 1.47, respectively, from 60 to 83 h of sintering, showing the 2223 phase is in equilibrium with Ca_2CuO_3 (seen as dark phases in Fig. 7, indicated as B); the ratio Bi/Pb increases from 5.11 to 5.26 over the same period, showing that the solubility of Pb decreases in 2212 and other non-superconducting phases and there is only insignificant evaporation of Pb during the annealing procedure. After 100 h sintering the Sr/Ca ratio reached again its maximum value of 1.00 and the Cu/Sr ratio remained constant at 1.47; showing that the 2223 phase is in equilibrium with $Sr_{14}Cu_{24}O_{41}$ and CuO. After 150 h decomposition of the 2223 phase proceeds further; the Sr/Ca ratio decreased to 0.91 from 1.00, the Cu/Sr ratio remained nearly constant at 1.46 and the Bi/Pb ratio increased to 5.41, indicating that the 2223 phase is in equilibrium with CuO and Ca_2CuO_3. For 197 h the Sr/Ca ratio decreased further to value 0.87, and the Cu/Sr and Bi/Pb ratio increased to 1.67 and to 5.46, respectively, indicating that the 2223 phase is in equilibrium with CuO and Ca_2CuO_3.

Fig. 3 presents a plot of $\ln[-\ln(1-C)]$ versus $\ln t$ for the 2223 phase formation reaction. It indicated a two-stage process with a marked change of the *n*-exponent during the course of the 2223 phase formation after 36 h sintering. At short sintering times ($t<60$ h) the slope, *n*, is 0.2. For 36 h $<t<60$ h, *n* is equal to 1. The values taken by *n* do not correspond strictly to one of those typical for the types of transformations listed above. This fact is not surprising since different types of reaction may proceed simultaneously. The values of the *n* for the first segment of the $\ln[-(1-C)]$ versus plots probably do not reflect the initial process of the transformation. The initial slope, n_1, close to 0.5, indicates that at this stage of the reaction, thickening of the 2223 plates after their edges have impinged is the main process occurring since the increase in 2223 amount is nearly 3 vol%, showing insignificant nucleation to have taken place (Fig. 2 and Fig. 4). Another explanation might

Table 2
The experimental data for the 2223 phase of the bulk Bi–Pb–Sr–Ca–Cu–O superconductors sintered at 850°C for 60 h in air, together with a calculated set of values

2Θ (°)	d_{obs} (Å)	d_{cal} [a] (Å)	h	k	l	I_{obs}
4.75	18.603	18.605	0	0	2	24
19.14	4.638	4.638	0	0	8	9
23.91	3.722	3.722	0	0	10	72
24.34	3.664	3.657	1	1	3	18
26.15	3.408	3.408	1	1	5	51
28.77	3.103	3.103	1	1	7	100
31.85	2.810	2.810	1	1	9	63
33.05	2.710	2.710	0	2	0	71
33.43	2.680	2.681	2	0	2	22
33.79	2.653	2.653	0	0	14	76
35.41	2.535	2.535	1	1	11	49
38.81	2.320	2.321	0	0	16	14
41.17	2.193	2.193	2	0	10	12
43.86	2.063	2.064	0	0	18	13
44.43	2.039	2.039	0	2	12	42
47.47	1.915	1.915	2	2	0	43
47.95	1.897	1.897	1	1	17	40
50.57	1.805	1.805	0	3	1	11
51.79	1.765	1.765	2	2	8	13
52.53	1.742	1.742	1	1	19	28
53.91	1.701	1.701	2	2	10	15
54.99	1.670	1.679	1	2	16	15
56.49	1.630	1.629	1	3	7	25
57.36	1.606	1.606	1	1	21	17
58.31	1.582	1.582	3	1	9	17
59.75	1.548	1.548	0	0	24	32

[a] Wavelength Cu Kα~1.542 Å.
a=3.779 Å, b=3.834 Å, c=37.154 Å.

be that due to the very high reactivity of the freeze-dried powder (nearly 75% of 2223 phase in 20 h of sintering) the nucleation took place in a very small time or was suppressed by the fast 2223-growth process. As mentioned above, the n values for medium sintering times (36 h$<t<$ 60 h), n_2, are nearly equal to 1. It is well known that the crystallites of the 2223 phase have a plate-like shape with high aspect ratio (length to thickness ratio) (Fig. 4). $n=1$, therefore, represents a pure 2-dimensional growth without a contribution from a thickening of crystallites.

The above results on the kinetics of the formation of 2223 are not valid only for the samples produced by the freeze-drying but also for the samples prepared by the methods employed in the references [39–41,53] such as two-powder and thermal co-decomposition routes. Fig. 5 describes the reaction kinetics for thermal co-decomposition plus the two-powder oxide route, in addition to the freeze-dry route [39,41,53]. Fig. 5 shows three different n values for the samples prepared by the thermal co-decomposition and two-powder methods (Table 3). For sintering between 20–36 h, n_1 values for the co-decomposition and two-powder routes are 0.7 and 0.2, respectively, indicating the growth of the already nucleated 2223 grains and thickening of the plates after their edges are in touch with each other, respectively (Fig. 6 and Fig. 7). For sintering between 36–60 h, n_2 is 0.2 for the samples

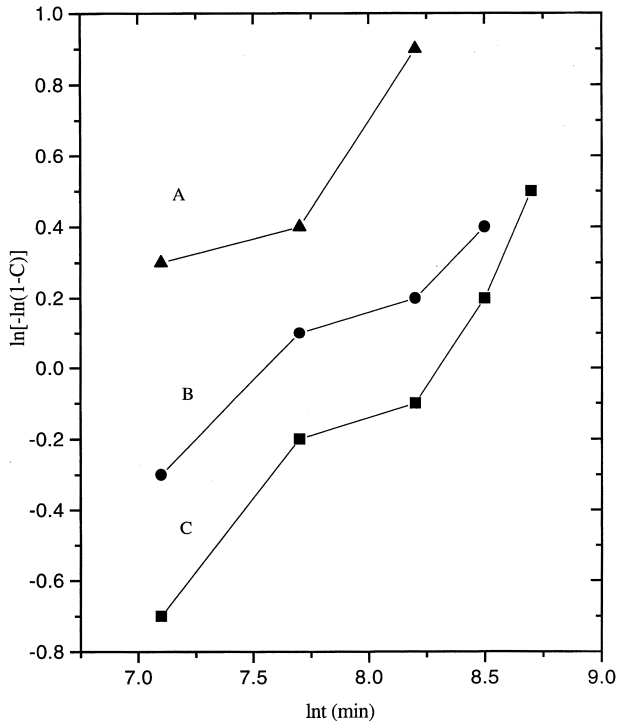

Fig. 5. Plot of ln[−ln(1−C)] versus ln t for the high-T_c phase formation for the bulk Bi–Pb–Sr–CaCu–O superconductors prepared by the (A) freeze-drying, (B) Thermal co-decompositon, (C) two-powder precursor powders.

produced by both methods, indicating the thickening of the plates grown already (Fig. 6 and Fig. 7). For sintering between 60 and 100 h, n_3 is 0.7 for the thermal co-decomposition samples, and 2 for the two-powder samples. The first value indicates continuation of the grain growth of the pre-existing 2223 grain via a–b planes confined by the matrix of 2212 plates grown in the c-direction [41], while the second one indicates the initial growth of the nucleates at a constant rate. The formation kinetics is therefore a multi-stage process in the samples produced by two-powder route, and thermal co-decomposition as well as in the case of the freeze-dried samples, i.e. both random-nucleation and growth occur in sintering at 850°C in air during formation of the 2223 phase.

In bulk samples, Zhu et al. [54] studied a nominal composition corresponding to

Table 3
The Avrami exponents of the bulk Bi–Pb–Sr–Ca–Cu–O superconductors prepared from the precursor powders produced by three different methods during formation

Production method	n_1 [a]	n_2 [b]	n_3 [c]
Freeze-drying	0.2	1	–
Thermal co-decomposition	0.7	0.2	0.7
Two-powder	0.83	0.2	2

[a] n values between 20–36 h sintering.
[b] n values between 36–60 h sintering.
[c] n values between 60–83 h sintering.

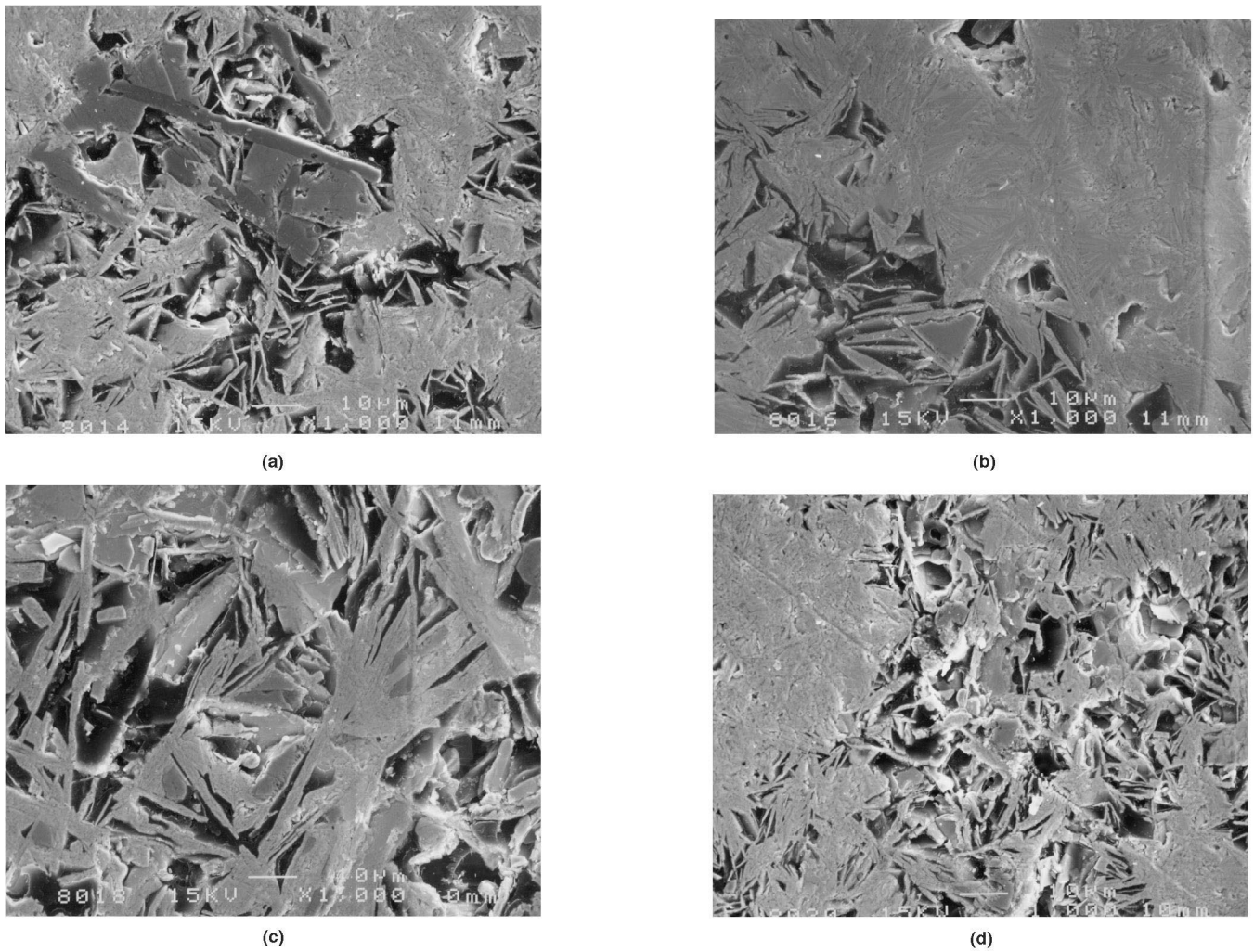

Fig. 6. SEM secondary electron micrographs of the bulk Bi–Pb–Sr–Ca–Cu–O superconductors prepared from the freeze-dried precursor powders sintered at 850°C in air for (a) 20 h, and mounted in a polymeric holder.

$Bi_{1.84}Pb_{0.34}Sr_{1.91}Ca_{2.03}Cu_{3.06}O_{10-y}$ by employing the (solid state) oxide route. They obtained *n*-values between 0.43 and 0.79 for sintering temperatures ranging from 840°C to 870°C and 7.5 h$<t<$35 h. Grivel et al. [36] has found *n* values between 1.2 and 0.63 at 857°C for 12$<t<$ 35 for a nominal composition $Bi_{1.83}Pb_{0.33}Sr_{1.93}Ca_{1.93}Cu_{3.00}O_{10-y}$.

Grivel and Flukiger [36] and Hu et al. [45], who used the (solid state) oxide route to prepare precursor powders for producing Ag-clad tapes, have shown that the *c*-axis texture degree is lower at the surface of the pellets for the 2223 phase than for the 2212 phase. The XRD patterns of Bi–Pb–Sr–Ca–Cu–O pellets made by freeze-dried powders for 20, 36, and 60 h (Fig. 2) and SEM micrographs [411 confirm these observations, where it is seen that the 2223 grains have some general alignment in the *a–b* plane (Fig. 4) and are confined in the early stages of formation by the plate-like matrix (2212) grown in cdirection (Fig. 4). Fig. 6 and the XRD pattern for 83 h sintering (Fig. 2) showed that decomposition of the 2223 into non superconducting (alkali earth cuprates) and 2212 had commenced as discussed above. From the SEM micrographs quasi-spherical liquid particles are seen, which are a mixture of Ca_2PbO_4 and non-superconducting phases [162, 183, 189] (indicated as L in Fig. 6). For 150 h, the mixture of 2212 plates (comparatively small in amount with respect to the 2223 grains) in the *c*-direction and the 2223 grains parallel to the *a–b* plane are seen in Fig. 4. For 197 h decomposition of the 2223 phase goes further. The random mixture of the 2212 plates and the 2223 grains in the *a–b* plane are seen in Fig. 4. The 2212 needles can be easily distinguished from the edges of the 2223 plates in SEM micrographs from Fig. 4. The grain-growth of the both 2223 and 2212 phases is seen in Fig. 4 and Fig. 7.

Four main phases, namely Ca_2CuO_3 (indicated as B in Fig. 6), $Sr_{14}Cu_{24}O_{41}$ (indicated as A in Fig. 6), 2212 (indicated as C in Fig. 6), 2223 (indicated as D in Fig. 6), are seen clearly in Fig. 6. Fig. 7 was obtained from the back-scattering SEM of polished samples seen in Fig. 6. The Ca_2CuO_3 phase observed is the darkest in colour, the

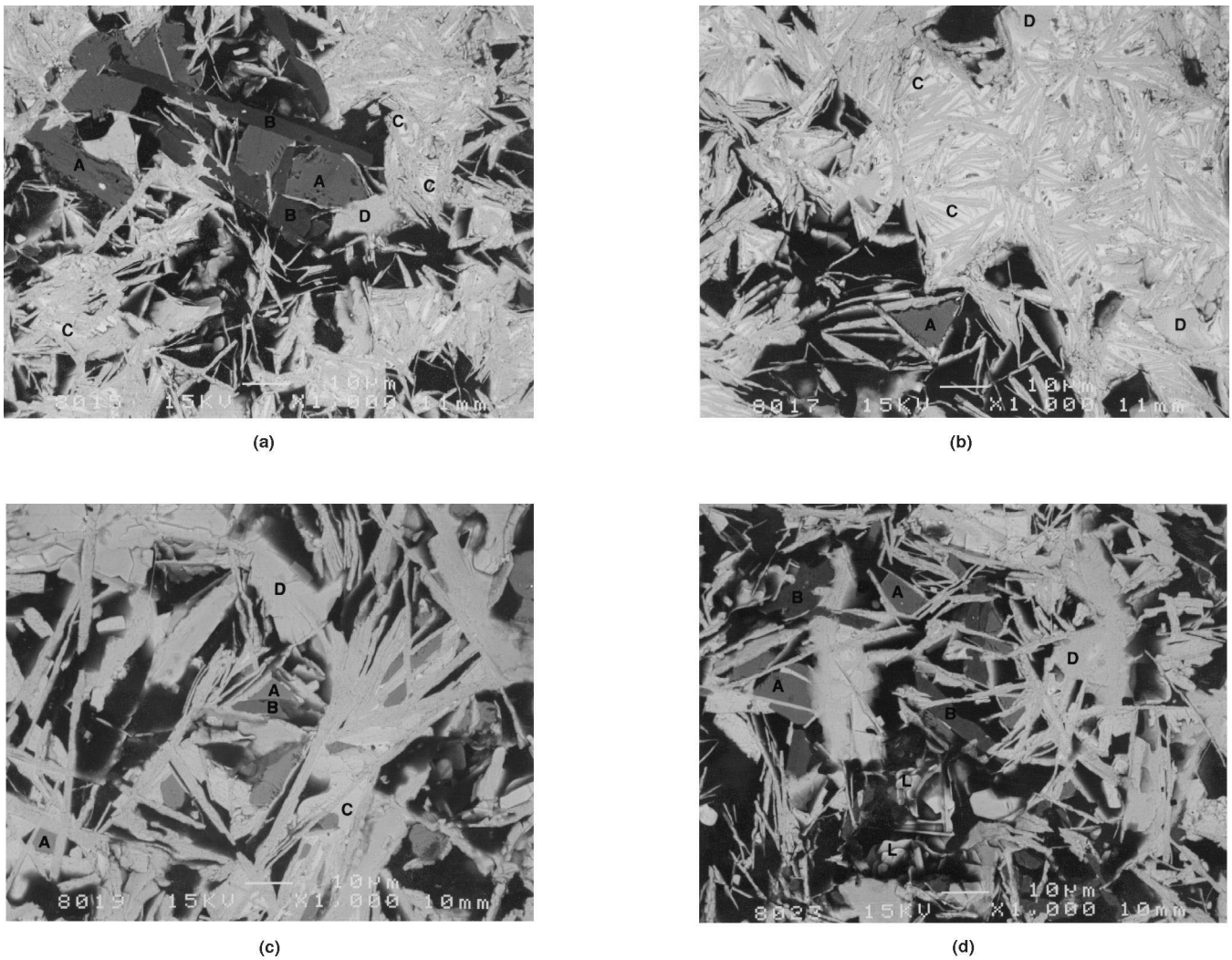

Fig. 7. Back-scattering SEM micrographs of the bulk Bi–Pb–Sr–Ca–Cu–O superconductors prepared from the freeze-dried precursor powders sintered at 850°C in air for (a) 20 h, (b) 36 h, (c) 60 h, (d) 83 h. The samples were polished but not etched, and mounted in a polymeric holder.

$Sr_{14}Cu_{24}O_{41}$ phase is having darker colour than the 2212, 2223, but lighter than the Ca_2CuO_3. The 2212 phase has the lightest colour (Fig. 7); the matrix is the 2223 phase.

Fig. 8 shows the chemical analyses profile of the phases Ca_2CuO_3 (Fig. 8), $Sr_{14}Cu_{24}O_{41}$ (Fig. 8), 2212 (Fig. 8), and 2223 (Fig. 8) seen in Fig. 6 and Fig. 7 (secondary and back-scattering images, respectively) by EDX obtained from the polished, unetched, and carbon-coated bulk Bi–Pb–Sr–Ca–Cu–O superconductor samples sintered at 850°C in air for 20, 36, 60, and 83 h.

Table 4 includes the exact composition of the four main phases, which was obtain from the EDX analysis of back scattering SEM of the polished samples. The other phases such as Ca_2PbO_4, liquid phase, and the CuO are in very small quantities and particle sizes (<1 micron) so that it is not possible to obtain their exact stoichiometric formulae since there is a severe limitation of the applicability of X-ray analysis in the SEM, EDX (energy dispersive analysis) due to electron scattering in the bulk of the specimen in a region ~1–2 microns in diameter [55].

4. Summary

It was shown here that the nucleation and the growth, which was confirmed as two-dimensional mechanism as indicated in previous works, rate were relatively fast between 0 and 36 h. At the final stage, between 36 and 60 h, because of the impingement of the growth fronts of different nuclei, the high formation rate of 2223 is suppressed. The major reactant 2212 remains as a solid and its plate-like configuration determines the two dimensional nature of the reaction. The amount of liquid forms during reaction is small.

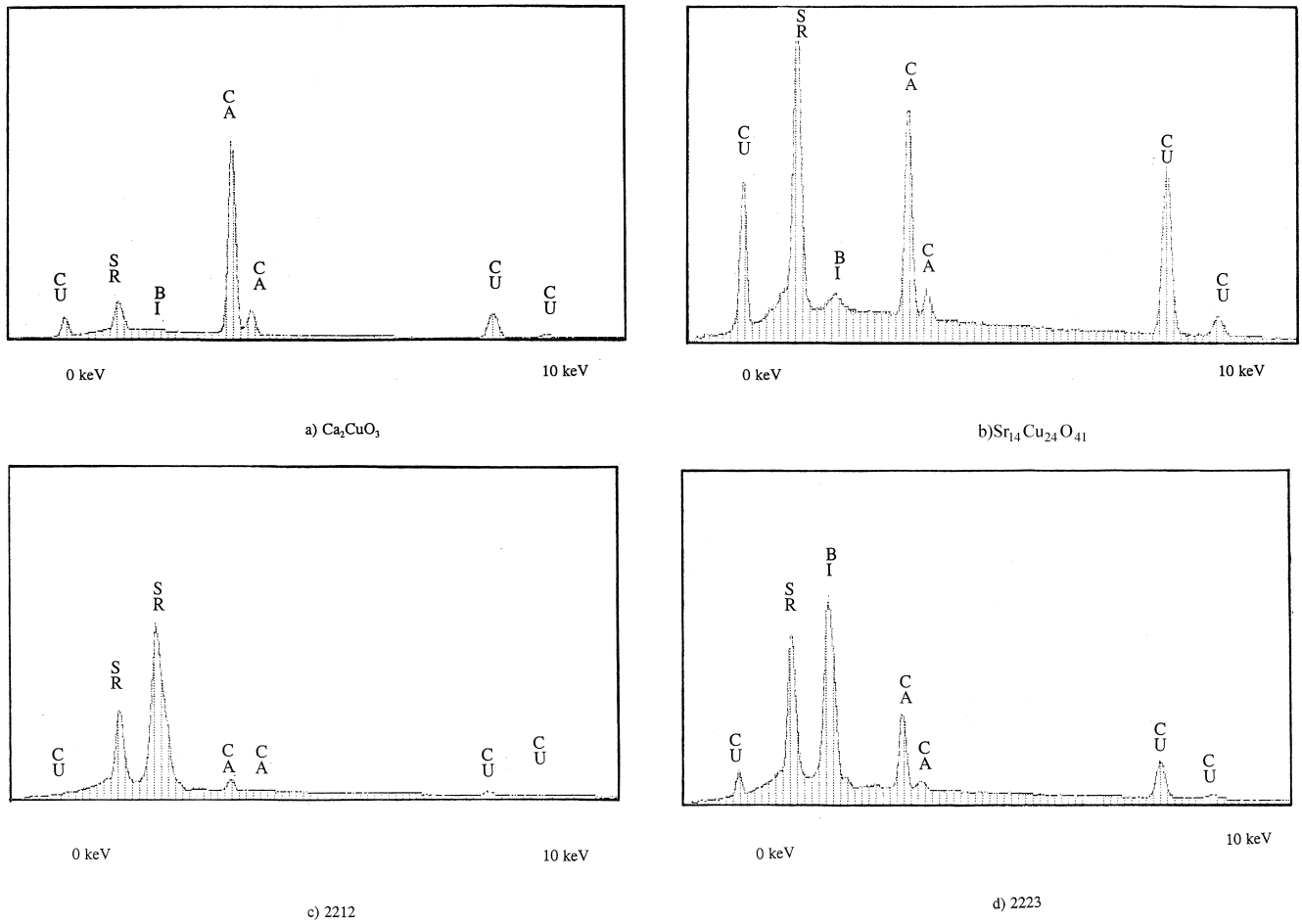

Fig. 8. Chemical analyses profile of the phases (a) Ca_2CuO_3, (b) $Sr_{14}Cu_{24}0_{41}$, (c) 2212, and (d) 2223 seen in Fig. 6 (secondary and back-scattering images, respectively) by EDX obtained superconductor samples sintered at 850°C in air for 20, 36, 60, and 83 h.

Table 4
The cation ratio of the phases Ca_2CuO_3, $5r_{14}Cu_{24}O_{41}$, 2212, and 2223 obtained by EDX from the samples sintered at 850°C in air for 20 h

Phase	Bi [a]	Pb	Sr	Ca	Cu	O
2212	1.3	0.9	1.8	1.1	2.2	8
2223	1.8	0.34	2.0	1.8	3.2	10.0
Ca_2CuO_3	0.0	0.0	0.2	1.8	1.0	3.0
$Sr_{14}Cu_{24}O_{41}$	0.2	0.1	7.5	7.4	25.0	41.0

[a] The above values are normalised to the values in the stoichiometric formulae.

References

[1] H. Nobumasa, K. Shimuzu, Y. Kitano, T. Kawai, Jpn. J. Appl. Phys. 27 (1988) L846.
[2] N. Kijima, H. Endo, J. Tsuchiya, A. Sumiyama, M. Mizuno, Y. Oguri, Jpn. J. Appl. Phys. 27 (1988) L1852.
[3] I. Matsubara, R. Funahashi, T. Ogura, H. Yamashita, Y. Uzawa, K. Tanizoe, T. Kawai, Physica C 218 (1993) 181.
[4] Y.L. Chen, R. Stevens, J. Am. Ceram. Soc. 75 (1992) 1142.
[5] Y.L. Chen, R. Stevens, J. Am. Ceram. Soc. 7 (1992) 1150.
[6] Y.L. Chen, R. Stevens, J. Am. Ceram. Soc. 75 (1992) 1160.
[7] Y. Ikeda, H. Ito, S. Shimomura, Z. Hiroi, M. Takano, Y. Bando, J. Takada, K. Oda, H. Kitaguchi, Y. Miura, Y. Takeda, Physica C 190 (1991) 18.
[8] P.E.D. Morgan, R.M. Housley, J.R. Porter, J.J. Ratto, Physica C 176 (1991) 279.
[9] J. Tsuchiya, H. Endo, N. Kijima, A. Sumiyama, M. Mizuno, Y. Oguri, Jpn. J. Appl. Phys. 29 (1989) L918.
[10] T. Hatano, K. Aota, S. Ikeda, K. Kakamura, K. Ogawa, Jpn. J. Appl. Phys. 27 (1988) L2055.
[11] M. Mizuno, H. Endou, J. Tsuchiya, N. Kijima, A. Sumiyama, Y. Oguri, Jpn. J. Appl. Phys. 2 (1988) L1225.
[12] D. Shi, M. Tang, M.S. Boley, M. Hash, K. Vandervoort, H. Claus, Y.N. Lwin, Phys. Rev. B 40 (1989) 2247.
[13] D. Shi, M. Boley, J.G. Chen, M. Xu, K. Vandervoort, Y.X. Liao, A. Zangvil, Appl. Phys. Lett. 5 (1989) 699.
[14] Q. Feng, H. Zhang, S. Feng, X. Zhu, K. Wu, Z. Liu, L. Xue, Solid State Commun. 78 (1991) 609.
[15] M. Wang, G. Xiong, X. Tang, Z. Hong, Physica C 210 (1993) 413.
[16] G. Zorn, B. Seebacher, B. Jobst, H. Gobel, Physica C 177 (1991) 494.
[17] H.K. Liu, S.X. Dou, Y.C. Guo, K.E. Easterling, X.G. Li, M. Mater. Res 6 (1991) 2287.
[18] M. Tatsumisago, C.A. Angell, Y. Akamatsu, S. Tsuboi, N. Tohge, T. Minami, Appl. Phys. Lett. 55 (1990) 699.

[19] T. Kamatsu, R. Sato, K. Imai, K. Matusita, T. Yamashita, Jpn. J. Appl. Phys. 27 (1988) L550.
[20] T. Komatsu, K. Imai, R. Sato, K. Matusita, T. Yamashita, Jpn. J. Appl. Phys. 27 (1988) L533.
[21] D.G. Hinks, L. Soderholm, D.W. Capone II, B. Dabrowski, A.W. Mitchell, D. Shi, Appl. Phys. Lett. 53 (1988) 423.
[22] A. Inoue, H. Kimura, K. Matsuzaki, A.-P. Tsai, T. Masumoto, Jpn. J. Appl. Phys. 27 (1988) L941.
[23] T. Minami, Y. Akamatsu, M. Tatsumisago, N. Tohge, Y. Kowada, Jpn. J. Appl. Phys. 27 (1988) L777.
[24] S.L. Yuan, S.Z. Jin, B. Zhu, W. Wang, J.Q. Zhang, G. Zheng, W. Guan, Mod. Phys. Lett. B 3 (1989) 331.
[25] T. Komatsu, R. Sato, K. Matusita, T. Yamashita, Jpn. J. Appl. Phys. 54 (1989) L1169.
[26] W. Wong–Ng, C.K. Chiang, S.W. Freiman, L.P. Cook, M.D. Hill, Ceram. Bull. August (1992) 1261.
[27] W. Wong–Ng, C.K. Chiang, S.W. Freiman, L.P. Cook, N.M. Hwang, M.D. Hill, Proceedings of the First Material Ceramic Science and Technology Congress, Anahelm, California, USA, 1990, p. 115.
[28] W. Wong-Ng, C.K. Chiang, S.W. Freiman, L.P. Cook, N.M. Hwang, M.D. Hill, Mater. Res. Soc. Symp. Proc. 169 (1990) 123.
[29] Y.T. Huang, R.G. Liu, S.W. Liu, P.T. Wu, W.N. Wang, Appl. Phys. Lett. 56 (1990) 779.
[30] Y.T. Huang, C.Y. Shel, W.N. Wang, C.K. Kiang, W.H. Lee, Physica C 169 (1990) 76.
[31] Y.S. Sung, E.E. Hellstrom, Physica C 253 (1995) 79.
[32] H. Kitaguchi, J. Takada, K. Oda, Y. Miura, J. Mater. Res. 5 (1990) 929.
[33] M. Avrami, J. Chem. Phys. 7 (1939) 1103.
[34] J.S. Luo, N. Merchant, V.A. Maroni, D.M. Gruen, B. Tani, W.L. Carter, G.N. Riley, K.H. Sandhage, Appl. Supercon. 1 (1993) 101.
[35] C.N.R. Rao, K.J. Rao, Phase Transitions in Solids, Mc-Graw Hill, 1978.
[36] J.-C. Grivel, R. Fliikiger, J. Alloys Comp., 1997.
[37] M. Avrami, J. Chem. Phys. 8 (1940) 212.
[38] M. Avrami, J. Chem. Phys. 9 (1941) 177.
[39] M. Yavuz, Ph.D. Thesis, University of Wollongong-Materials Engineering Department, p. 237, p. xviii, 1997.
[40] Y.C. Guo, J.N. Li, M. Yavuz, H.K. Liu, E.R. Vance, S.X. Dou, Adv. Cryogen. Eng. 42 (1995) 751.
[41] M. Yavuz, H. Maeda, E.R. Vance, H.K. Liu, S.X. Dou, submitted to J. of Supercond. Sci. and Tech.
[42] N.L. Wu, T.C. Wei, S.Y. Hou, S.Y. Wong, J. Mater. Res. 5 (1990) 2056.
[43] R. Liang, H. Ishii, H. Kawaji, M. Itoh, T. Nakamura, Jpn. J. Appl. Phys 29 (1990) L1412.
[44] A. Nozue, H. Nasu, K. Kamiya, Jpn. J. Appl. Phys. 28 (1989) L2161.
[45] Q.Y. Hu, H.K. Liu, S.X. Dou, Physica C 250 (1995) 7.
[46] P. Majewski, S. Kaesche, F. Aldinger, Adv. Mater. 8–9 (1996) 762.
[47] K. Schultze, P. Majewski, B. Hettich, G. Petzow, Z. Metallkd. 81 (1990) 836.
[48] S.X. Dou, H.K. Liu, C.C. Sorrell, K.-H. Song, M.H. Apperley, S.J. Guo, K.E. Easterling, W.K. Jones, Mater. Forum 14 (1990) 92.
[49] Y. Ikeda, H. Ito, S. Shimomuro, Z. Hiroi, M. Takano, Y. Bando, J. Takada, K. Oda, H. Kitaguchi, Y. Miura, Y. Takeda, T. Takada, Physica C 190 (1991) 18.
[50] Y. Yamada, B. Oberst, R. Flukiger, Supercond. Sci. Technol. 4 (1991) 165.
[51] Y.L. Chen, R. Stevens, J. Am. Ceram. Soc. 75 (1992) 1150.
[52] P. Majewski, S. Kaesche, F. Aldinger, J. Am. Ceram. Soc., 1997.
[53] M. Yavuz, H. Maeda, E.R. Vance, H.K. Liu, S.X. Dou, submitted to J. of Supercond. Sci. and Tech.
[54] J.-C. Grivel, R. Flukiger, Supercond. Sci. Technol., 1997.
[55] D.B. Williams, Practical Analytical Electron Microscopy in Materials Science, chap. 1, Verlag–chemie International, 1985, p. 4.